

R.V. Budny et al.

# Alpha Heating in JET Plasmas with Sawteeth

(22nd June 2015 – 26th June 2015)  
Lisbon, Portugal

“This document is intended for publication in the open literature. It is made available on the clear understanding that it may not be further circulated and extracts or references may not be published prior to publication of the original when applicable, or without the consent of the Publications Officer, EUROfusion Programme Management Unit, Culham Science Centre, Abingdon, Oxon, OX14 3DB, UK or e-mail [Publications.Officer@euro-fusion.org](mailto:Publications.Officer@euro-fusion.org)”.

“Enquiries about Copyright and reproduction should be addressed to the Publications Officer, EUROfusion Programme Management Unit, Culham Science Centre, Abingdon, Oxon, OX14 3DB, UK or e-mail [Publications.Officer@euro-fusion.org](mailto:Publications.Officer@euro-fusion.org)”.

The contents of this preprint and all other EUROfusion Preprints, Reports and Conference Papers are available to view online free at <http://www.euro-fusionscipub.org>. This site has full search facilities and e-mail alert options. In the JET specific papers the diagrams contained within the PDFs on this site are hyperlinked.

# Alpha heating in JET plasmas with sawteeth

R.V. Budny<sup>a</sup> and JET contributors<sup>b</sup>

*EUROfusion Consortium, JET, Culham Science Centre, Abingdon, OX14 3DB, UK*

Alpha heating is essential for practical energy production from DT fusion reactions. Experiments to detect alpha heating were performed in TFTR (1994) [1] and in JET (1997) [2]. Measurements of alpha heating were difficult since the alpha heating power  $p_\alpha$  was small relative to the external heating  $p_{\text{ext}}$ , and since the experiments were not accurately reproducible. It was difficult to realize comparable DD or TT discharges for comparison. One cause of irreproducibility in the JET discharges was the presence of sawteeth.

This paper studies effects of sawteeth in the discharges featured in [2]. They had  $I_p=3.8\text{MA}$  and  $B_{\text{tor}}=3.6\text{T}$ , and density 35% of the Greenwald empirical limit. The mix of D and T was varied from discharge to discharge by changing the D and T in the neutral beam injection while maintaining their total powers approximately constant ( $P_{\text{NB}} \simeq 10.3\text{MW}$ ). Several of them had global fusion power to heating power ratio  $Q_{\text{DT}}=0.7$ , and core values (defined in [3]) of 1.2. These are near the highest values seen in JET. The fraction of T to total beam power  $f_{\text{T}}=P_{\text{T-NB}}/(P_{\text{NB}})$  is an important metric for the scans. Here, one with D-only, three with D and T, and two with T-only NB [2] are used. Summary values are in Table I.

Sawtooth crashes cause rapid drops in the core electron temperature  $T_e$ . Minor disruptions also cause rapid crashes, but sawtooth crashes have simultaneous rapid increases in  $T_e$  outside the mixing radius (past the radius where the safety factor is unity). Crash times were determined from core electron cyclotron measurements of  $T_e$ . Examples are shown in Fig. 1-a). The pattern of frequent small sawteeth crashes petering off after the start of NB is typically seen in JET discharges. Even large sawtooth crashes within the first second of NB did not appear to have major effects on the later performance. However, larger crashes occurring later in the phase of stored energy ramp-up did have significant impacts, discussed below. Sawtooth crashes were generally seen in TFTR supershots continuing briefly into the NB phase, but they were usually suppressed later during the NB phase. Effects of the sawtooth crashes in the JET scan can be seen on the total neutron emission rate  $S_n$  and on the central neutron emission rate  $s_n(0)$  observed in fits to neutron camera measurements in Fig. 1-b).

The electron density profiles  $n_e$  were sometimes hollow, as often seen during the JET DT campaign. The general trend was for the  $n_e$  shape to vary from peaked for H to flatish for D to increasing peakedness in DT and T H-mode plasmas [4]. For this reason, and also since the heating directly affects the stored energy, it is insightful to focus on the electron and ion energy densities  $w_e$  and  $w_i$ .

At least in the core,  $w_e$  and  $n_e$  increased approximately linearly in time from the start of NB for at least 1.6s. Plots of  $w_e$  volume-averaged from the magnetic axis to  $x(\equiv \text{square-root of the$

normalized toroidal flux) = 0.2 in Fig. 1-c) show  $w_e$  increasing with approximately the same rate except for abrupt decreases at sawtooth crashes. They do not show a clear trend in  $s_n(0)$  or  $f_T$  suggesting that  $p_\alpha$  is not playing a significant role, perhaps due to systematic changes in confinement or energy loss rates compensating for increased  $p_\alpha$ . The values for  $w_i$  shown in Fig. 1-d) do show a trend of increasing  $f_T$  suggesting that an isotopic effect might be playing a role if 43011 is excluded. This discharge had the most hollow  $n_e$  and recycling rates 50% higher than the others. The  $n_e$  pedestal was the lowest and the  $T_i$  and  $T_e$  pedestals the highest in the scan. This discharge was pivotal for the argument against isotopic mass effects in [2].

The  $T_e$  profiles also are similar across the scan at the same time, and do not exhibit consistent trends in  $f_T$  or  $s_n(0)$  up to the times of the first significant sawtooth crash as shown in Figs. 2-a). At later times sawtooth crashes break the tight clustering of rates and the discharges that have not crashed continue to increase at the same growth rates. By 14s a clear separation of  $T_e$  and  $T_i$  profiles appear with the high  $s_n(0)$  shots, still before sawtooth crashes, having the highest  $T_e$  and  $T_i$ . Profiles of  $T_i$  shown in Figs. 2-b) and Figs. 2-d) show greater separation. Central values of  $T_e$  shown in [2] just before the last sawtooth crashes did have clear separation with  $S_n$ . This separation of  $T_e$  can be attributed to the sawtooth crashes and ion-electron coupling  $p_{ie}$ . Increased sawtooth period with increasing  $f_T$  has been reported [5].

The discharges were modeled using the TRANSP code to study heating and transport. The modeling achieves approximate agreement with  $S_n$  and  $s_n(0)$ , as well as with the EFIT diamagnetic energy indicating that the modeling is approximately accurate. The largest discrepancy between the simulated and measured  $s_n(0)$  differed by at most 12% at the peak, indicating that  $p_\alpha$  is credible. The sawtooth crashes are modeled assuming Kadomtsev helical mixing of current and fast ions at the observed sawtooth crash times. Sawtooth crashes have been observed to mix fast beam and alpha ions [6]. The core volume-averaged  $p_\alpha$ , fast alpha density  $n_\alpha$  and pressure  $\beta_\alpha$  also increase approximately linearly in time, except for sharp breaks at sawtooth crashes. At 13.6s the predicted peak core averaged  $p_\alpha$  is half the maximum calculated for this scan. In 42856 at 14.1s the peak predicted ratio  $p_\alpha/p_{ext}$  is near 0.2.

The electron channel time-integrated the beam fueling and electron heating source rates during the energy ramp-up phase. The rates of increases of the volume-integrated  $n_e(x)$  and the volume- and time-integrated NB electron source rates within  $x$  are nearly equal. The agreement of rates holds both for the core ( $x \simeq 0.2$ ) and larger  $x$ , suggesting that the TRANSP beam deposition calculation is accurate and the electron flux is negligible, or that an inward pinch and outward diffusivity transport were canceling each other.

Similarly the volume integrated electron energy  $\int_0^1 dV w_e$  increased at a constant rate  $\simeq 2\text{MW}$  throughout the ramp-up. TRANSP uses measurements to calculate the heating and loss profiles. The dominant terms for electrons are  $p_e \equiv p_{be} + p_\alpha + p_{oh} + p_{ie} - p_{conde} - p_{conve}$ . The radiation emission profile  $p_{rad}$  is not available, so TRANSP is used to predict the line, bremsstrahlung,

and synchrotron emission. Their total volume-integrated rates scale in time approximately as the measured total emission, but are lower by about a factor of 0.8. The convected and conducted power losses  $p_{\text{conde}}$  and  $p_{\text{conv}_e}$  are TRANSP outputs. To study  $p_\alpha$  consider core  $\int_0^x dV w_e \simeq \int_0^x \int_{12}^t dt dV p_e$  integrated to  $x=0.2$  or  $0.3$ . This is dominated by  $p_{\text{be}}$ . During the end of the ramp-up and into the flat-top phases the terms  $p_{\text{oh}}$ ,  $p_{\text{rad}}$ ,  $p_{\text{ie}}$ ,  $p_{\text{conde}}$ ,  $p_{\text{conv}_e}$ , and  $p_\alpha$  contribute roughly equally, except for the  $f_T=0$  discharge where  $p_\alpha$  is negligible. This makes it difficult to accurately quantify  $p_\alpha$ . The total thermal ion stored energy  $\int dV w_i$  increased at the same rate, also  $\simeq 2\text{MW}$ . The dominate terms are:  $p_i \equiv p_{\text{bi}} - p_{\text{ie}} - p_{\text{cx}} - p_{\text{cond}_i} - p_{\text{conv}_i}$ . One large uncertainty is the charge-exchange loss term  $p_{\text{cx}}$  which is estimated (from the estimated recycling rate) to be large near the edge. The  $p_{\text{cond}_i}$  and  $p_{\text{conv}_i}$  terms are large. In the mid-radius region near 13.6s  $\chi_i$  is around  $0.5 \text{ m}^2/\text{s}$  and  $\chi_e$  is less.

An important parameter from the modeling is the hydrogenic isotopic mass  $\langle A \rangle$  defined as  $(n_{\text{H}}+2n_{\text{D}}+3n_{\text{T}})/(n_{\text{H}}+n_{\text{D}}+n_{\text{T}})$ . This is calculated from species conservation using the beam neutral ionization rates and the wall recycling and gas fueling rates [7]. The core  $\langle A \rangle$  is dominated by the beam neutral ionization rates. Across the scan  $\langle A \rangle \simeq f_T + 2$ . The time delay  $\delta_t$  is another important parameter. Values in Table I tend to increase with  $f_T$  and  $\langle A \rangle$  as shown in Figs. 3-a). Neither  $S_n$  nor  $p_\alpha$  are linearly correlated with  $\delta_t$  as shown in Figs. 3-b). This suggests that increasing core isotopic mass is the cause of longer  $\delta_t$ , and thus contributing to the higher core  $T_e$  and  $T_i$ .

In conclusion  $\langle A \rangle$  is strongly correlated with the increase of  $\delta_t$ , and the delayed crashes allowed  $T_e$  and  $T_i$  to obtain higher values. At constant time  $T_i$  was higher for discharges with higher  $\langle A \rangle$ . Thus longer  $\delta_t$  and  $p_{\text{ie}}$  could explain the higher  $T_e$ . The computed  $p_\alpha/p_{\text{ext}}$  is up to 0.2, but electron power balance in the core shows that multiple terms with uncertainties are comparable to  $p_\alpha$ .

Work supported in part by the US DoE contract No. DE-ACO2-76-CHO3073, and carried out within the framework of the EUROfusion Consortium, and has received funding from the Euratom research and training programme 2014-2018 under grant agreement No 633053. The views and opinions expressed herein do not necessarily reflect those of the European Commission.

<sup>a</sup>Princeton University, Princeton, NJ 08543, USA

<sup>b</sup> See the Appendix of F. Romanelli, *et al.*, Proceedings of the 25th IAEA Fusion Energy Conference 2014, Saint Petersburg, Russia.

- [1] G.Taylor, J.D.Strachan, R.V.Budny, and D.R.Ernst, Phys. Review Lett. **76** 2722 (1996).
- [2] P.R. Thomas, P Andrew, B.Balet, D. Bartlett, J. Bull, B.de Esch, *et al.*, Phys. Review Lett. **80** 5548 (1998)
- [3] R.V.Budny, J.G.Cordey, "Core fusion power gain and alpha heating in JET, TFTR, and ITER", to be submitted
- [4] R.V.Budny, D.R. Ernst, T.S.Hahm, D.C.McCune, J.G.Cordey, *et al.*, Phys of Plasmas, **7** 5038 (2000)
- [5] M.F.F. Nave, N.N. Gorelenkov, K.G. McClements, S.J. Allfrey, *et al.*, Nucl. Fusion **42** 281 (2001)
- [6] G McKee, R.Fonck, B.Stratton, R.Bell, R.Budny, C. Bush, B. Grek, *et al.*, Phys. Review Lett. **75** 649 (1995)
- [7] R.V.Budny, M.G.Bell, D.K.Mansfield, J.D.Strachan, S.Zweben, *et al.*, 21<sup>st</sup> EPS, Montpellier, France (1994)

Discharge	$f_T$	$\delta_t$ [s]	$\langle A \rangle$ (14.0s)	$p_\alpha$ [ $10^{-2}$ MW/m <sup>3</sup> ]	$n_\alpha$ [ $10^{17}$ /m <sup>3</sup> ]
40365	0.0	0.9026	1.99	0.0	0.0
42870	0.27	0.9515	2.24	2.1	0.38
42856	0.52	1.4565	2.55	4.7	1.02
42847	0.88	1.4015	2.49	3.6	0.88
42840	1.00	1.6100	2.77	2.1	0.40
43011	1.00	1.6217	2.91	0.7	0.17

Table 1:  $f_T$ , time delay  $\delta_t$  to 1st significant crash, core (volume-averaged to  $x=0.2$ ) hydrogenic mass,  $p_\alpha$  and number of fast alpha ions before the 1st significant crash.

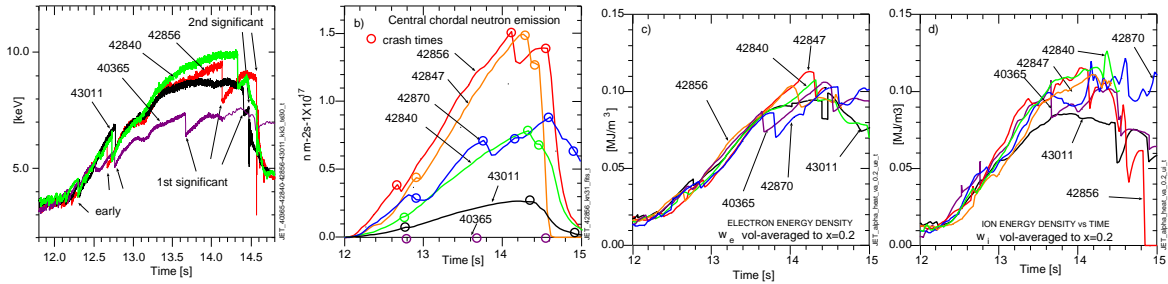


Figure 1: a) Examples of sawtooth / minor disruption crashes in ECE signals of the discharges with  $f_T = 0.0, 0.52$ , and  $1.0$  from the alpha heating scan; significant crashes / minor disruptions seen after 13.6s; b) Sawtooth crash effects in the measured central chordal neutron emission rates; Time evolution of the core volume-averaged c) electron and d) thermal ion energies.

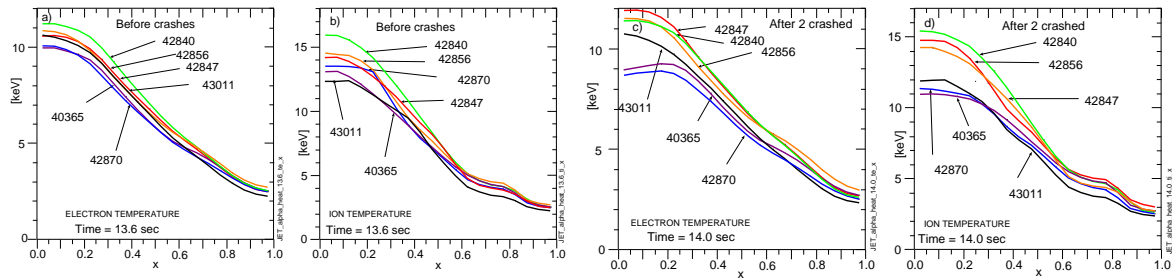


Figure 2: Profiles of  $T_e$  and  $T_i$  profiles at 13.6s (before the first significant sawtooth crash) and 14.0s (after two of the discharges experienced their first significant sawtooth crash).

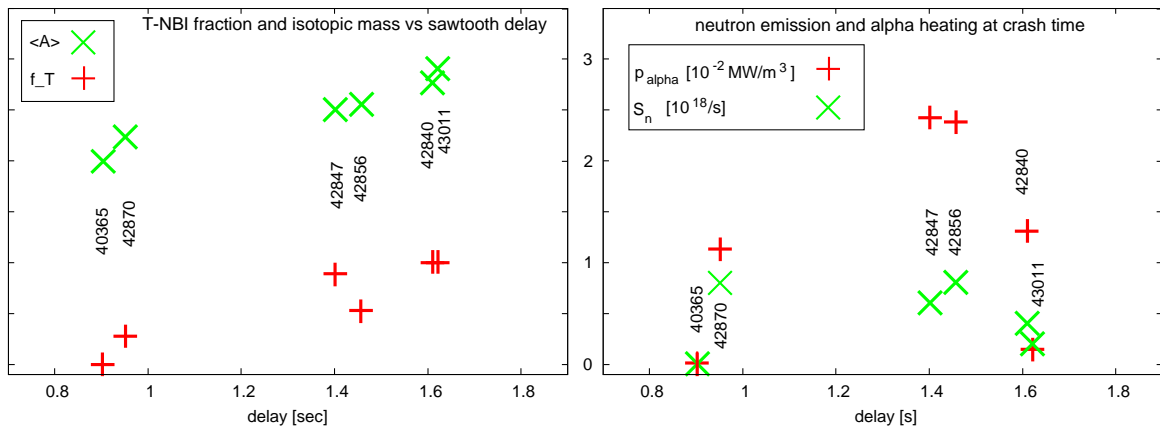


Figure 3: Correlations of delay times to the first significant sawtooth crash with a) core hydrogenic mass and tritium fraction of NB power; b) neutron emission and core alpha heating at the 1st significant crash times.